Solid Freeform Fabrication 2021: Proceedings of the 32nd Annual International Solid Freeform Fabrication Symposium – An Additive Manufacturing Conference
Reviewed Paper

Rotational Digital Light Processing for Edible Scaffold Fabrication

Alexis Garrett [1], Arian Jaberi [1], Auston Viotto [1], Ruiguo Yang [1], Ali Tamayol [1,2], Ajay Malshe [3], Michael P. Sealy [1,*]

[1]Mechanical and Materials Engineering Dept., University of Nebraska, Lincoln, NE 68588, USA
[2]Dept. of Biomedical Engineering, University of Connecticut, Storrs, CT 06269, USA
[3]School of Mechanical Engineering, Purdue University, West Lafayette, IN, 47907, USA

Abstract

A key hurdle to overcome in the development of alternative meat-based protein is the manipulation of mechanical or mastic properties of the 3D scaffolds. These properties influence the mouth feel of the product and must be tunable to achieve a variety of meat analogous textures. The goal of this research was to investigate a printing technology hypothesized to enable textural adjustment in alternative proteins. In pursuit of this goal, a novel digital light processing (DLP) printer with a rotational collector plate was developed to enable radially cured layers with the ability to incorporate multi-material composite structures. The purpose of this research was to quantify the effect of cured layer orientation on the bulk mechanical properties of (gelatin methacryloyl) GelMA scaffolds. In addition, current photocrosslinking systems do not emphasize the edibility of the materials used in the process. Tartrazine, an edible photo-absorber, was investigated in its use for improving print resolution during the crosslinking process.

Keywords: edible, polymer, cellular agriculture, photolithography

1. Introduction

A recent push experienced in the food industry as well as in environmental efforts is for meat-based protein production methods alternative to traditional livestock rearing. In order to increase overall meat production, the ability to mimic the intended meat product in an efficient method is a key metric for success[1]. This requires a high level of understanding and manipulability of the cellular behavior in the artificial tissue system as well as the manufacturing methods to create these tissues to control the overall structural properties of the product. This in turn requires significant scientific advancements in cellular biology and the manufacturing methodology utilized for the production process.

Skeletal or striated muscle consists of bundles of thousands of muscle fibers connected via the extracellular matrix (ECM) that serves as a natural scaffold for the muscle tissue [2]. This extracellular matrix - primarily made up of collagen, enzymes, and glycoproteins - is crucial to

[1]* Email: sealy@unl.edu | Phone +1 (402) 472-1659

cell adhesion and migration within the tissue and helps to regulate the cellular growth, metabolism, and differentiation exhibited by the attached cells [3]. In addition, marbling of muscle tissue with intermittent fatty regions further increases the complexity of the structure, both in material composition and regional structural properties [4]. This complex material and structural variation must be mimicked in a cultivated meat to achieve higher order textures within the product.

Although basic culturing techniques have been established for the components for tissue engineering and many manufacturing methods for 3-dimensional tissue scaffolds have been developed, these methods are still in their infancy and focus on the cellular behavior rather than the experiential aspects of the tissue construct, such as successfully controlling the directional mechanical behavior or degree of anisotropy within the thick constructs. These methods range widely from scaffoldless systems [5], three dimensional printable structures, decellularized natural extracellular matrices from plant sources [6], and many more novel approaches. One method that has been investigated in its ability to control the degree of anisotropy is through an extrusion-based printing of PCL, a medical grade polymer, and the incorporation of intermittent layers of electrospun PCL nanofibers [7]. This hybrid technology shows significant potential in giving way to increasing the controllability of the directional mechanical behaviors under loading.

Hydrogel scaffolds show particular promise in their cellular compatibility as well as their inherent tailorability in composition and handling to adjust the overall properties of the material, including pore sizing and printing resolution [8]. GelMA, a widely used hydrogel for biomedical engineering studies is a gelatin based hydrogel which is biocompatible, biodegradable [9]. It has been used for a variety of tissue engineering and scaffold-based printings using different manufacturing processes such as extrusion based, stereolithography, microfluidic, etc. GelMA based scaffold was using for culturing and differentiating of muscle cells with the extrusion based pen printer [10]. In order to improve the resolution within the printed structure and increase the printing time window, an edible photo-absorber such as tartrazine- a yellow food dye- can be incorporated, which will absorb the light, reducing unintended crosslinking from light bleeding into the pre-hydrogel material [11].

Finally, the development of a novel manufacturing process which has the ability to incorporate variations of materials and processing within the printing cycle would serve as a crucial step in the development of a process that allows for the controlled placement of materials and structural properties in a three-dimensional space. A novel stereolithographic printing process that incorporated multiple materials within the same print [12] could be directly tailored for the use of stereolithographic curing of GelMA in which multiple vats with varied material concentrations and cell types could be used to create regional changes in the printed structure. To further allow for increased layering control, the development of a rotational collection system allows for these structures to be defined in polar coordinate systems. In this way, materials or their printing parameters could be adjusted radially rather than in a 2-dimensional planar schematic to control the variation of materials in a more core and sheath-like methodology. When scaling up to a mass production capacity, this layer by layer control would lead to both material and processing tunability and even reel-to-reel systems in which an additional structure could be cured within the scaffold, as described previously with extrusion and electrospinning. The development of this process, however, requires the understanding of fluid dynamics and its effect on the printing system to optimize its function [13].

2. Materials and Methods

2.1 Development of a hybrid stereolithography apparatus for meat analogs tissue printing

In order to engineer tissue analogous to the high order texture found in meat, we designed a custom hybrid stereolithographic apparatus to print anisotropic layers. The apparatus is a combination of a digital light projector (DLP) stereolithographic printer with a novice cylindrical continuously rotating build-plate as shown in Fig. 1a. This design of the rotational DLP printer was chosen to allow for additional mechanisms for adjustment in the scaffold itself and its overall mechanical properties, including the incorporation of a secondary material system such as electrospun fiber structures for a composite structure and designed failure behavior under stress. These structures will ultimately be chosen to mimic the shape of meat tissue and previous hydrogel-based scaffolds produced by digital light processing based on further works[11]. Examples of the Layer-by-Layer method and the Radial-Layer method are presented in Fig. 1b. An image of the first few layers is shown in Fig 1c.

A conventional DLP printer works by dipping a flat build-plate into a resin bath or VAT. The accuracy and thickness of the z layers are directly related to the precision of the stepper motor driving the z-axis stage. A projector then displays the current layer into the bottom of the VAT and curing the resin between the VAT and the build-plate. The build-plate will be raised to allow for more resin to flow for the next layer to be cured; this process repeating until the completion of the print. This rotating digital photolithographic method prototyped offers additional variations that are not available in the traditional layer orientations. The build-plate in the proposed system is a continuous rotating cylinder that is only partially dipped into the VAT. The build-plate rotates at 38 RPMs to drag resin up out of the VAT to cover the cylinder. The projector is then able to cure the thin layer of resin that coats the cylinder above the VAT. This layer and its thickness is controlled by the boundary layer conditions of the formed resin layer by the rotating cylinder and the non-slip condition at the body/resin interface [13]. Layer thickness is affected by the speed at which the stepper motor is driven, the viscosity of the resin, and the drag created by the cylinder. Though identified as variables, these were kept as constants for this proof of concept work.

Our hybrid DLP printer, seen in Fig. 1a, is made up of 4 main components including the microcontroller, z-axis linear actuator, rotational stepper motor, and VAT with DLP projector. The microcontroller is a RAMBo 1.3 mini (RAMBo; UltiMachine, South Pittsburg, TN) which runs the linear actuator, stepper motor, and limit switch. The RAMBo is running a custom firmware. The z-axis linear actuator (TBSM11; Applied Motion Products, Watsonville, CA) carries the rotational stage (1mm/revolution). The rotating motor is a NEMA 11-size hybrid bipolar stepping motor with a 1.8° step angle (200 steps/revolution) that is electronically 1/8th stepped using the microcontroller. The rotating motor drives a round belt and pulley system to rotate the High-Density Polyethylene (HDPE). The linear actuator lowers the cylinder about a quarter into the resin, hitting the limit switch.

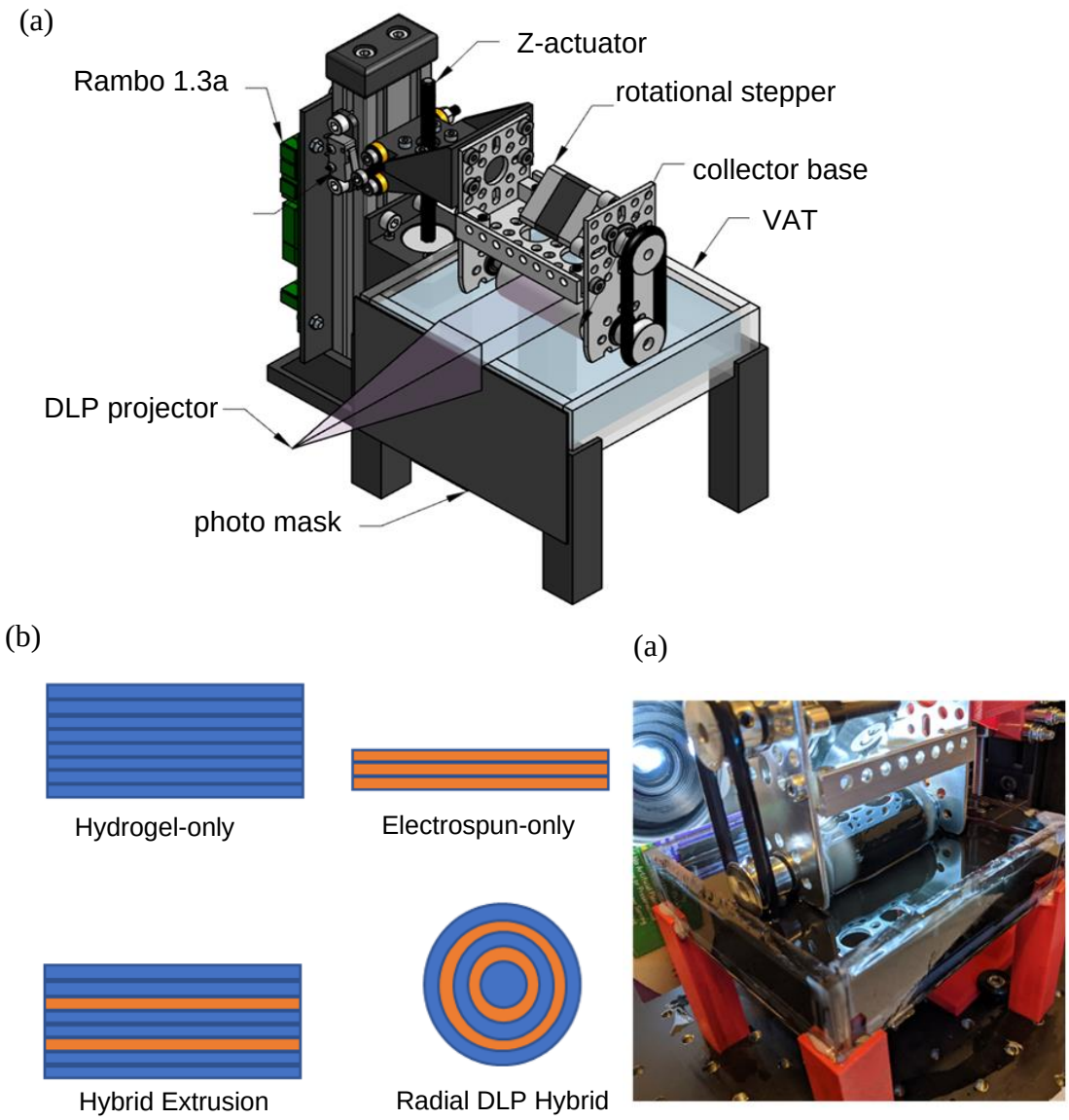

Fig. 1 (a) CAD model of DLP Rotational UV Manufacturing printer (DRUM). (b) Layer cross-sections for Hydrogel (blue) and Electrospun fiber sheets (orange) for layer-by-layer and Radial-Layer prints. (c) Image of the DRUM printer during operation.

2.2 Hydrogel preparation

GelMA was used as the hydrogel material for hydrogel printing purposes. GelMA was synthesized following a previously reported protocol [9]. For the synthesis, gelatin was dissolved in phosphate buffered solution (PBS, Gibco 14190235, Waltham, MA) with the ratio of 10% (w/v) at 50℃. Methacryloyl anhydride (MA) (Sigma Aldrich, St. Louis, MO) was added dropwise into the dissolved gelatin at a final concentration of 1.25%(v/v) and allowed to react for 1 hour. Upon reaction completion, the solution was diluted to a 5X PBS dilution with warm (40 ℃ to halt the

reaction. The diluted solution was transferred into a dialysis tube (12-14 kDa molecular weight cutoff) into deionized water to remove unreacted methacrylic anhydride from the solution for 5-7 days, or until the pH of the water remained stable. Finally, the GelMA solution was lyophilized at -80℃ for up to 7 days. For experiments, lyophilized GelMA was dissolved at varied concentrations in PBS and a solution of lithium acylphosphinate salt (LAP) (Allevi, Boston, MA) at a concentration of 0.067% (w/v)[10] .

2.3 Compression testing

Stock solutions of 7% w/V GelMA were prepared as previously described with set concentrations of tartrazine (0 mM and 1mM). A 100 uL volume of the stock solution was deposited onto the center of the lower compression plate and cured via UV stylus at a distance of 5 cm from the droplet surface. A sirloin steak cut was procured from a local butcher and frozen at -8 ℃ for 24 h. The sirloin samples were then prepared by slicing the specimen into 1.5 mm thickness slices and stamping a circular pattern using a metal cutting template which gave a final sample diameter of 11.5 mm. Each sample type was prepared in triplicate, at minimum. All compression testing was conducted using the CellScale Univert set to a 10 second loading period and a 5 second hold period, followed by a 5 second release period which cycled 3 times per sample with no dwell time between cycles. The samples were kept at ambient room temperature of 20.5 ℃ throughout the course of the compression testing period.

3. Results and Discussion

3.1 Printability of the DRUM printer

A baseline understanding of this proposed system is required for the evaluation of the potential of future manufacturing of complex shapes and the incorporation of complex structures such as electrospun scaffolds. As seen in Fig. 2, 5 samples were designed to gather this baseline functionality. The first was printed using the traditional layer-by-layer process as a control to compare to the prints of the four radial-layer orientations. Fig. 2a represents the image displayed by the digital light projector. Fig. 2b represents the actual 3D printed sample created by the above projections, respectively. Visual inspections of form accuracy such as radial, median, and cross-section deviations are covered for the various samples.

The sample **(i)** was created using the B9 Creator, layer by layer, with a print duration of 3 hours and a dimensional resolution of 30 microns. The sample has nearly flat and smooth top and bottom portions of the print, with relatively smooth side walls, as expected. Individual print layers are distinguishable along the outer wall. The print is also most nearly radially symmetric, with less than .1mm deviation between the X and Y axis, and no deviations along the median line or cross-section.

Sample **(ii)** was the first print processed on the DRUM system. The first test used a Polylactic Acid (PLA) drum manufactured through fused filament fabrication (FFF). The exposure projection was a static cube to print a cylinder. This print failed after extended exposure periods

of 4+ hours with little deposition of material. Different drum submersion depths and a variety of stepper motor speeds were tested through these trials. Prolonged exposure with a UV pen was able to grow a very small layer. No cured resin particulates could be located within the resin VAT which informed that the initial issue was surface wettability and uncured resin collection on the cylinder's surface. To address this issue with the following samples, the cylinder was adjusted to HDPE with improved surface wettability or interactivity with the resin. Two additional possible causes for the poor wettability is resin fouling or acid in the PLA negatively affecting the cross-linking of the resin, preventing curing.

Sample **(iii)** was the first print created using the HDPE cylinder, with an exposure pattern initiated as a wide rectangle covering the entirety of the build area. After a visible collection was deposited, 10 minutes, the projection pattern was reduced by 50% width and allowed to cure for an additional 10 minutes. This print shows that we are able to create stepped portions along the drum. The primary hypothesis for the non-uniform surface features exhibited in this print is the inconsistency in the boundary layers of the fluid flow induced by the cylinder and it's effect on uniform resin distribution. As each layer is built on itself, these inconsistencies can compound themselves, emphasizing that an optimization in the materials selection, rotational speed, and curing parameters are required for the optimal print resolutions. Additional testing would need to be done, however this effect should only affect larger prints as the radius increases requiring additional time to cure if rotational velocity is held constant [13].

The fourth sample's **(iv)** exposure pattern was the same as the second sample **(ii)**. The print shape was similar to sample **(i)** and was completed in 10 minutes. The print's top and bottom edges were rounded yet well defined. Two potential solutions to improving the sharpness of the corners are to use a gradient pattern with the light intensity of the image to allow the edges higher intensity exposure, allowing the resin to cure more uniformly across the build area or to reduce the distance 25 cm from the projector to the collector surface. Individual print layers are not visible, both due to the lost resolution problem previously mentioned and additionally attributed to the thickness of the resin deposited per revolution, yet to be investigated. The outer wall of the cylinder is very smooth, and the cylindrical print was nearly radially symmetric with respect to the true radial axis with less than 0.1 mm deviation between the X and Y axis, comparable with the B9 Creator printed part. No deviations along the median line or cross-section other than the top and bottom edges were noted.

The fifth sample's **(v)** exposure pattern was a three band build area to ensure control of the curing regions along the length of the cylinder. It was observed that less cured resin was found on the thin inner band than the outer bands, again contributed to the fluid dynamics of the cylinder pulling through the vat and the inconsistency in uncured resin deposits. The edges of the bands were thinner than the center of the band as seen by the roundings of each area, however the band edges were well defined with no curing outside the intended pattern. The resin must meet a certain threshold of light intensity to begin curing, and as the initial parameters such as projection intensity and rotational speed remain constant, the velocity at the surface of the print increases as the radius is increased by the deposited material. As this meets the threshold for photocuring time, the resin will no longer experience enough UV exposure to cure. Increased light energy on the outer portions of a pattern wall or adjusting the rotational speed as a function of the print percent completion may help evenly build up future patterns.

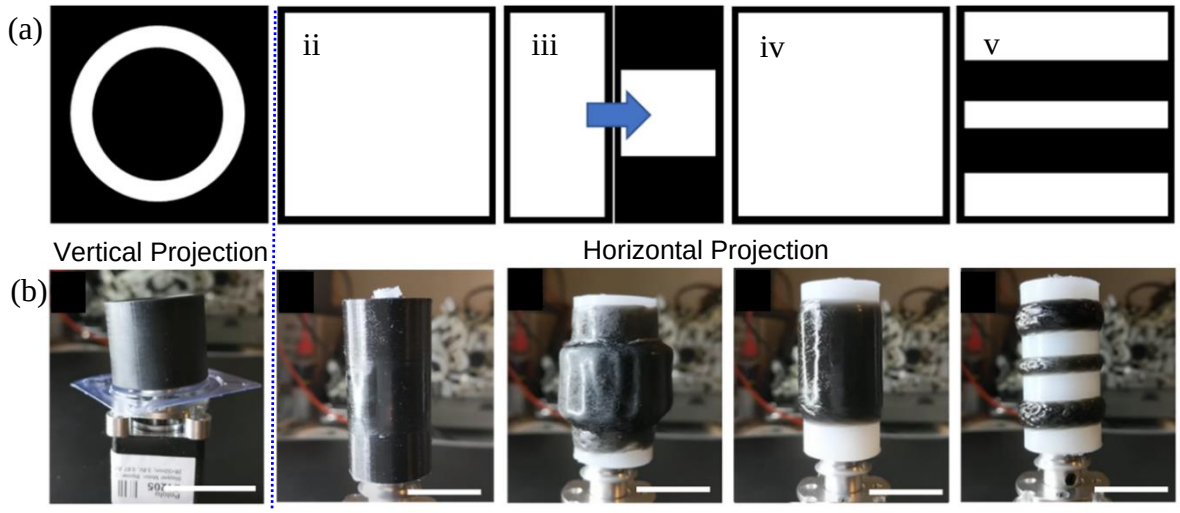

Fig. 2 DLP printed resin-based structures. (a) patterns of the projected sketch. (b) printed structures **(i)** B9 printed (ii, iii, iv, v) DRUM printed. Scale bar: b, 25 mm.

3.2 Compression study on hydrogel and meat

As can be seen in Fig. 3a, the compression stress of the hydrogels with or without the tartrazine, the photo-absorber, has been studied, these data were compared with the compression stress data of the sirloin meat. According to these results, UV curing duration has an effect on the maximum compression stress. The compression stress range for the GelMA 7% combined with 0,067% LAP was between 6 kPa for 0.25 minutes of UV irradiation, up to an average of about 90 kPa for the duration of 1 and 3 minutes of UV irradiation. These results demonstrate that increases in the UV duration cause an increase in maximum compression stress (Fig. 3b). Another set of results was conducted on the GelMA 7% with 0.067% of LAP and 1mM of tartrazine, on these set of experiment, as the tartrazine absorb the power of the UV irradiation, the curing duration was set for 3 and 5 minutes. These results demonstrate that the average of the maximum compression stress for the GelMA with tartrazine and curing time of 3 minutes was about 0.5 kPa, and the maximum compression stress for the GelMA with tartrazine with the UV curing of 3 minutes was about 1 kPa. Based on these data, the increase in compression stress due to the increase in UV duration was observed (Fig. 3c).

Sirloin steak was tested utilizing the same loading cycles as that of the GelMA. The sirloin samples were prepared as previously described with two key orientations, against the natural grain orientation of the skeletal muscle fibers and at an angle 45 degrees from the grain direction. The maximum compressive stress experienced in the 45-degree samples was approximately 45 kPa whereas the maximum experience by the against-the-grain samples was 35 kPa (Fig. 3d). Unexpectedly, the results from the grain orientation within the sample exhibited little effect on the behavior in compression. This could be due to the small sample size in which the anisotropy is not as well captured in compression as a thicker sample may exhibit.

As can be seen, the compression stress of the meat was similar to the compression result of the GelMA without tartrazine with a curing duration of about 1 and 3 minutes. These results demonstrate that GelMA can be a reasonable hydrogel for mimicking the mechanical behavior of the cultured cells in the hydrogel. For using the tartrazine there should be future studies on the compression stress of the GelMA with different concentrations and even with longer duration of UV, and there is the possibility that hybrid hydrogels can improve the mechanical property and curing time of the hydrogel, which will develop the compatible environment for the cell culturing and cellular differentiation.

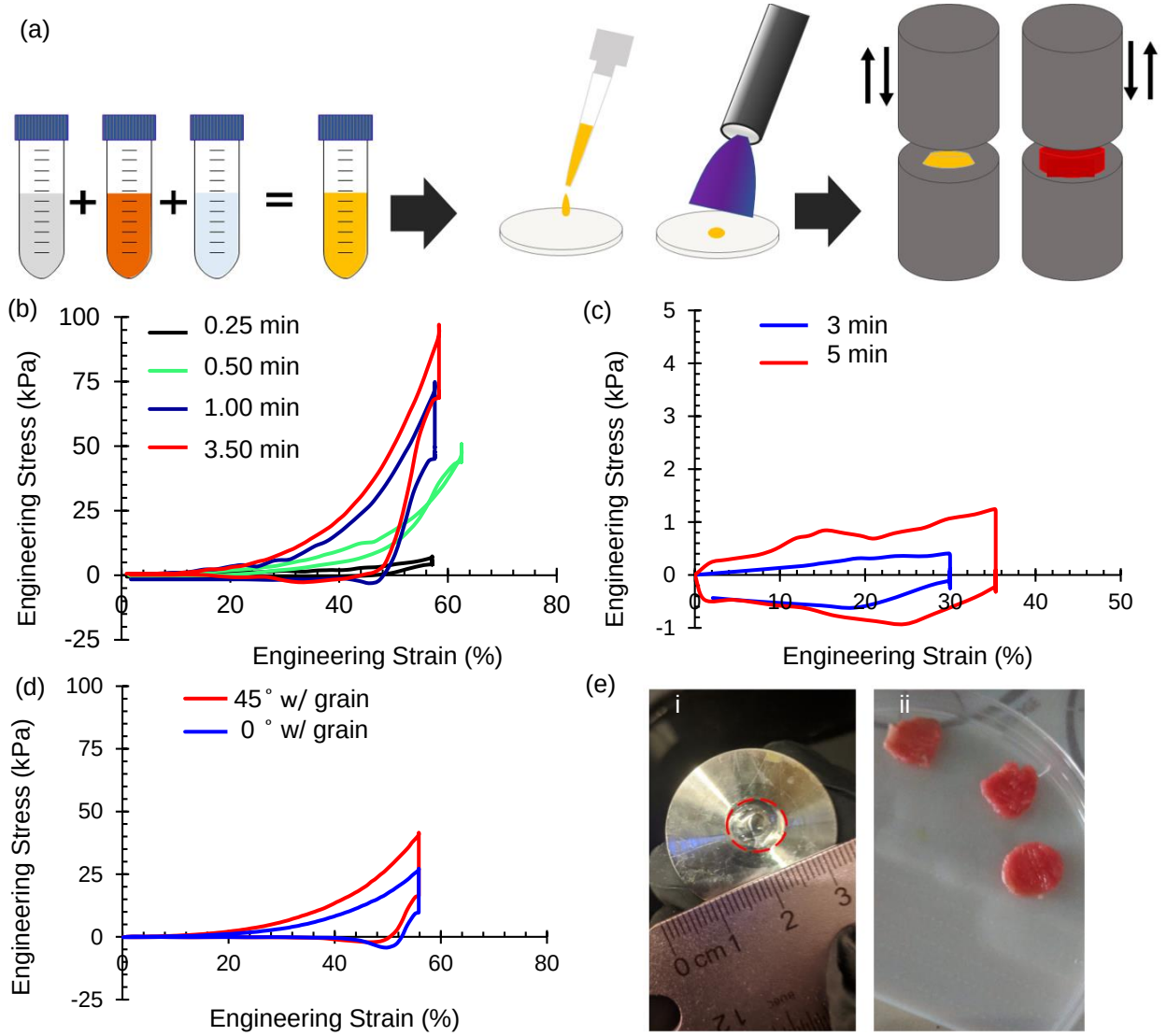

Fig. 3 Compression test on the GelMA hydrogel and meat. (a) schematic of the process for compression testing. (b) the engineering stress versus the strain rate of sirloin samples. (c) the engineering stress versus the strain rate of GelMA without tartrazine for the duration of 0, 0.25, 0.5, 1, and 3 minutes of UV during. (d) the engineering stress versus the strain rate of the GelMA with 1 mM of tartrazine for the duration of 3 and 5 minutes of UV curing. (e) images of the samples before the compression test (i) GelMA (ii) meat.

4. Conclusions and Future Work

After many iterations, a printer was successfully developed that allows for the curing of a traditional polymer resin in a radial layer orientation. A functional bioink, composed of PBS, GelMA, tartrazine, and LAP, was assessed in compression to validate its use with respect to mimicking a sirloin beef steak product. This ink will be tested in the developed printer system to determine optimal print parameters.

The ability to print defined internal architectures within the radially cured sample must be investigated to further validate the ability to successfully incorporate vascular paths to increase cell survival and proliferation in the scaffold structure. The incorporation of intermittent radial layers of electrospun scaffolding fibers to control the induced anisotropic mechanical behavior under varying loads should also be investigated. A key consideration in successfully incorporating a second material into a process involving photo-crosslinking is to ensure that the materials incorporated are crosslinkable to the hydrogel itself. It must also be perfusable by the pre-hydrogel solution to ensure the electrospun layer adheres to the previous layer. If you are unable to crosslink between the layers, you will have significant delaminations present between layers, unable to achieve the desired sample architecture. This will require significant optimization, both of the hydrogel and its printing parameters as well as the additional incorporated material and its preparation methodology.

In addition, the rotational path of crosslinking created by the DRUM system will induce a natural shearing force by the drag force experienced from the rotation of the drum in the viscous pre-hydrogel solution during the printing process. The presence of shear force has previously been shown to help in the alignment of the muscle cells within the hydrogel structure. This increased alignment is likely to also improve the rate of differentiation and proliferation that the embedded cells will exhibit, more quickly and effectively forming myotubular structures [10]. To further investigate the hypotheses held on the effects the DRUM fabrication will have on cellular behavior, testing of cell proliferation, differentiation, and protein expression must be conducted to quantify. After the scaffolds and fabrication process is characterized biologically, a more informed conclusion can be made on its ability to be used in mass cultivated meat production with the control over the mechanical behavior of the product itself.

Acknowledgments

This research was conducted as part of an undergraduate/graduate investigative research course in additive manufacturing in the Department of Mechanical and Materials Engineering at UNL Spring of 2020. This activity was partially supported by NSF CMMI: 1846478 and New Harvest.

References

1. Post, M. J., Cultured meat from stem cells: Challenges and prospects. *Meat Science* 2012, *92* (3), 297-301.

2. Alberts B, J. A., Lewis J, et al., Molecular Biology of the Cell. 4th edition. New York: Garland Science; 2002. *Genesis, Modulation, and Regeneration of Skeletal Muscle*. Available from: https://www.ncbi.nlm.nih.gov/books/NBK26853/
3. Deleon, K. Y.; Yabluchanskiy, A.; Winniford, M. D.; Lange, R. A.; Chilton, R. J.; Lindsey, M. L., 3 - Modifying matrix remodeling to prevent heart failure. In *Cardiac Regeneration and Repair*, Li, R.-K.; Weisel, R. D., Eds. Woodhead Publishing: 2014; pp 41-60.
4. Specht, E. A.; Welch, D. R.; Rees Clayton, E. M.; Lagally, C. D., Opportunities for applying biomedical production and manufacturing methods to the development of the clean meat industry. *Biochemical Engineering Journal* 2018, *132*, 161-168.
5. DuRaine, G. D.; Brown, W. E.; Hu, J. C.; Athanasiou, K. A., Emergence of scaffold-free approaches for tissue engineering musculoskeletal cartilages. *Annals of biomedical engineering* 2015, *43* (3), 543-554.
6. Gershlak, J. R.; Hernandez, S.; Fontana, G.; Perreault, L. R.; Hansen, K. J.; Larson, S. A.; Binder, B. Y. K.; Dolivo, D. M.; Yang, T.; Dominko, T.; Rolle, M. W.; Weathers, P. J.; Medina-Bolivar, F.; Cramer, C. L.; Murphy, W. L.; Gaudette, G. R., Crossing kingdoms: Using decellularized plants as perfusable tissue engineering scaffolds. *Biomaterials* 2017, *125*, 13-22.
7. Yang, G.-H.; Mun, F.; Kim, G., Direct electrospinning writing for producing 3D hybrid constructs consisting of microfibers and macro-struts for tissue engineering. *Chemical Engineering Journal* 2016, *288*, 648-658.
8. Lee, B. H.; Shirahama, H.; Kim, M. H.; Lee, J. H.; Cho, N.-J.; Tan, L. P., Colloidal templating of highly ordered gelatin methacryloyl-based hydrogel platforms for three-dimensional tissue analogues. *NPG Asia Materials* 2017, *9* (7), e412-e412.
9. Yue, K.; Trujillo-de Santiago, G.; Alvarez, M. M.; Tamayol, A.; Annabi, N.; Khademhosseini, A., Synthesis, properties, and biomedical applications of gelatin methacryloyl (GelMA) hydrogels. *Biomaterials* 2015, *73*, 254-271.
10. Russell, C. S.; Mostafavi, A.; Quint, J. P.; Panayi, A. C.; Baldino, K.; Williams, T. J.; Daubendiek, J. G.; Hugo Sánchez, V.; Bonick, Z.; Trujillo-Miranda, M.; Shin, S. R.; Pourquie, O.; Salehi, S.; Sinha, I.; Tamayol, A., In Situ Printing of Adhesive Hydrogel Scaffolds for the Treatment of Skeletal Muscle Injuries. *ACS Applied Bio Materials* 2020, *3* (3), 1568-1579.
11. Grigoryan, B.; Paulsen, S. J.; Corbett, D. C.; Sazer, D. W.; Fortin, C. L.; Zaita, A. J.; Greenfield, P. T.; Calafat, N. J.; Gounley, J. P.; Ta, A. H.; Johansson, F.; Randles, A.; Rosenkrantz, J. E.; Louis-Rosenberg, J. D.; Galie, P. A.; Stevens, K. R.; Miller, J. S., Multivascular networks and functional intravascular topologies within biocompatible hydrogels. *Science* 2019, *364* (6439), 458.
12. Choi, J.-W.; Kim, H.-C.; Wicker, R., Multi-material stereolithography. *Journal of Materials Processing Technology* 2011, *211* (3), 318-328.
13. Childs, P. R. N., Chapter 6 - Rotating Cylinders, Annuli, and Spheres. In *Rotating Flow*, Childs, P. R. N., Ed. Butterworth-Heinemann: Oxford, 2011; pp 177-247.